J|A|C|S
ARTICLES
Published on Web 11/26/2003

$M_2(hpp)_4Cl_2$ and $M_2(hpp)_4$, Where M = Mo and W: Preparations, Structure and Bonding, and Comparisons with C_2, C_2H_2, and C_2Cl_2 and the Hypothetical Molecules $M_2(hpp)_4(H)_2$†

Malcolm H. Chisholm,*,‡ Judith Gallucci,‡ Christopher M. Hadad,*,‡ John C. Huffman,§ and Paul J. Wilson‡,||

Contribution from the Department of Chemistry, The Ohio State University, 100 West 18th Avenue, Columbus, Ohio 43210, the Department of Chemistry, Indiana University, 800 East Kirkwood Avenue, Bloomington, Indiana 47405, and the Department of Chemistry, University of Bath, Claverton Down, Bath BA2 7AY, UK

Received February 12, 2003; E-mail: chisholm@chemistry.ohio-state.edu; hadad@chemistry.ohio-state.edu

Abstract: The reaction between $M_2Cl_2(NMe_2)_4$, where M = Mo or W, and Hhpp (8 equiv) in a solid-state melt reaction at 150 °C yields the compounds $M_2(hpp)_4Cl_2$ **1a** (M = Mo) and **1b** (M = W), respectively, by the elimination of $HNMe_2$ [hpp is the anion derived from deprotonation of 1,3,4,6,7,8-hexahydro-2*H*-pyrimido-[1,2-*a*]pyrimidine, Hhpp]. Purification of **1a** and **1b** is achieved by sublimation of the excess Hhpp and subsequent recrystallization from either CH_2Cl_2 or $CHCl_3$ (or $CDCl_3$). By single-crystal X-ray crystallography, the structures of **1a** and **1b** are shown to contain a central paddlewheel-like $M_2(hpp)_4$ core with Mo−Mo = 2.1708(8) Å (from CH_2Cl_2), 2.1574(5) Å (from $CDCl_3$), W−W = 2.2328(2) Å (from $CDCl_3$), and M−N = 2.09(1) (av) Å. The Cl ligands are axially ligated (linear Cl−M−M−Cl) with abnormally long M−Cl bond distances that, in turn, depend on the presence or absence of hydrogen bonding to chloroform. The quadruply bonded compounds $M_2(hpp)_4$, **2a** (M = Mo), and **2b** (M = W), can be prepared from the reactions between 1,2-$M_2R_2(NMe_2)_4$ compounds, where R = *t*Bu or *p*-tolyl, and Hhpp (4 equiv) in benzene by ligand replacement and reductive elimination. The compounds **2a** and **2b** are readily oxidized, and in chloroform they react to form **1a** and **1b**, respectively. The electronic structure and bonding in the compounds **1a**, **1b**, **2a**, and **2b** have been investigated using gradient corrected density functional theory employing Gaussian 98. The bonding in the M−M quadruply bonded compounds, **2a** and **2b**, reveals M−M δ^2 HOMOs and extensive mixing of M−M π and nitrogen ligand lone-pair orbitals in a manner qualitatively similar to that of the M_2-(formamidinates)$_4$. The calculations indicate that in the chloride compounds, **1a** and **1b**, the HOMO is strongly M−Cl σ antibonding and weakly M−M σ bonding in character. Formally there is a M−M triple bond of configuration $\pi^4\sigma^2$, and the LUMO is the M−M δ orbital. An interesting mixing of M−M and M−Cl π interactions occurs, and an enlightening analogy emerges between these d^4−d^4 and d^3−d^3 dinuclear compounds and the bonding in C_2, C_2H_2, and C_2Cl_2, which is interrogated herein by simple theoretical calculations together with the potential bonding in axially ligated compounds where strongly covalent M−X bonds are present. The latter were represented by the model compounds $M_2(hpp)_4(H)_2$. On the basis of calculations, we estimate the reactions $M_2(hpp)_4 + X_2$ to give $M_2(hpp)_4X_2$ to be enthalpically favorable for X = Cl but not for X = H. These results are discussed in terms of the recent work of Cotton and Murillo and our attempts to prepare parallel-linked oligomers of the type [[bridge]−[M_2]−]$_n$.

Introduction

Our attempts to prepare parallel and perpendicular one-dimensional polymers/oligomers of the type represented schematically by **I** and **II**, respectively, incorporating M−M quadruple bonds with attendant carboxylate ligands have been thwarted by facile ligand scrambling reactions involving the carboxylates.[1,2]

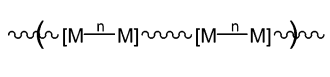

I

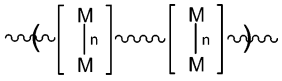

II

The scrambling of carboxylate groups can occur by either adventitious free carboxylic acid[3] or by intermolecular exchange

† Part of this work has previously been communicated at the 220th National Meeting of the American Chemical Society, Washington DC, August 20−24, 2000; INOR-531.

‡ Department of Chemistry, The Ohio State University, 100 West 18th Avenue, Columbus, OH 43210.

§ Department of Chemistry, Indiana University, 800 East Kirkwood Avenue, Bloomington, IN 47405.

|| Department of Chemistry, University of Bath, Claverton Down, Bath, BA2 7AY, UK.

(1) Chisholm, M. H. *Acc. Chem. Res.* **2000**, *33*, 53−61.
(2) Cayton, R. H.; Chisholm, M. H.; Huffman, J. C.; Lobkovsky, E. B. *J. Am. Chem. Soc.* **1991**, *113*, 8709−8724.

10.1021/ja0301065 CCC: $25.00

due to oxygen lone-pair to metal interactions.[4] We previously noted that the compound $Mo_2(form)_2(CH_3CN)_4(BF_4)_2$, where form = PhNCHNPh, **III**, can be used as a scavenger for adventitious free carboxylate anion or carboxylic acid and thus shuts down carboxylate exchange.[5] However, it then became apparent that the selection of a ligand such as a formamidinate in the first place would avoid ligand scrambling since its nitrogen lone-pairs are relatively inert with respect to intermolecular bonding. Recently, Cotton and Murillo have taken good advantage of this fact in the synthesis and characterization of dicarboxylate-bridged dinuclear compounds of the type $(form)_3M_2(\mu\text{-bridge})M_2(form)_3$,[6] (dimer of dimers) along with cyclotrimers $[(form)_2M_2(\mu\text{-bridge})]_3$ and cyclotetramers (squares), $[(form)_2M_2(bridge)]_4$, where form = ArNCHNAr.[7−9] In these cyclic structures, the bridges are in *cis*-positions as a result of the *trans*-influence order N > O. Thus, the formamidinate ligand may not prove suitable for the preparation of dicarboxylate-bridged one-dimensional polymers of the type depicted by **II**. On the other hand, the parallel polymers of type **I** could be accessible if the bridging group was not sterically demanding and sufficiently long so as to prevent steric congestion between neighboring M_2 units. Bearing this in mind, we recognized that the hpp ligand, where hpp is the anion derived from deprotonation of 1,3,4,6,7,8-hexahydro-2*H*-pyrimido[1,2-*a*]pyrimidine, Hhpp, **IV**, might circumvent the problems associated with ligand exchange and could comply with the steric requirements noted above. Indeed, from considerations of molecular packing, it should be possible to synthesize a chain of the type shown in **V**.

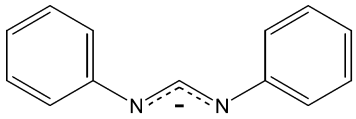

III

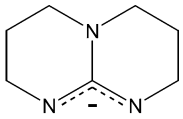

IV

—[M≡M]—C≡C—[M≡M]—C≡C—[M≡M]— **V**

We describe here our high-yield syntheses of $M_2(hpp)_4Cl_2$ compounds, where M = Mo and W, which are potential synthons for the development of this type of chemistry, together with reactions which yield $M_2(hpp)_4$. Alternate preparations of $Mo_2(hpp)_4$,[10,11] $W_2(hpp)_4Cl_2$,[12] and syntheses of $W_2(hpp)_4 \cdot 2NaHBEt_3$[13] and $W_2(hpp)_4$[14] have been recently reported by Cotton and Murillo. The electronic structure of these compounds, as determined by density functional theory calculations, is also reported along with that for the hypothetical molecules $M_2(hpp)_4(H)_2$, and a comparison is made with the bonding in C_2, C_2H_2, and C_2Cl_2.

Results and Discussion

Syntheses. $M_2(hpp)_4Cl_2$. The free ligand Hhpp (8 equiv) and the readily available $M_2Cl_2(NMe_2)_4$ (M = Mo or W) compounds are combined, finely ground in a drybox, and then placed in a sublimation apparatus. Then, under an inert argon atmosphere, the mixture is heated on the bench at 150 °C, melt conditions, for ca. 12−15 h, during which time $HNMe_2$ is evolved. The color change from orange to brown accompanies the transformation of $M_2Cl_2(NMe_2)_4$ to $M_2(hpp)_4Cl_2$. The excess Hhpp is then removed by sublimation at ca. 150 °C, 10^{-4} Torr. These melt reactions produce $M_2(hpp)_4Cl_2$ in quantitative yield as judged by ^{1}H NMR spectroscopy. Purification by recrystallization from dichloromethane yields $Mo_2(hpp)_4Cl_2$, **1a** and $W_2(hpp)_4Cl_2$, **1b**, the former having CH_2Cl_2 in the lattice as determined by single-crystal X-ray diffraction studies. Subsequent recrystallization from chloroform gives crystals **1a**·$6CHCl_3$ and **1b**·$6CHCl_3$. A summary of crystallographic data is given in Table 1, and NMR spectroscopic data are given in the Experimental Section.

$M_2(hpp)_4$. These compounds are readily prepared from the reactions between 1,2-$M_2R_2(NMe_2)_4$ and Hhpp (4 equiv) in benzene at room temperature with prolonged stirring (3 days) at room temperature when R = ^{i}Bu and *p*-tolyl.[15,16] These reactions proceed via the stepwise substitution of NMe_2 for hpp and subsequent reductive elimination. From reactions carried out in NMR tubes, we observe that the compounds where R = ^{i}Bu eliminate isobutane and isobutylene and where R = *p*-tolyl the biaryl coupling product is observed.

The previously reported preparation of $Mo_2(hpp)_4$, **2a**, by Cotton, Murillo, and co-workers was via the reaction between $Mo_2(O_2CCF_3)_4$ and Lihpp (4 equiv) in toluene which gave a 22% isolated yield,[10] although this was later optimized to 73% by changing the solvent to tetrahydrofuran.[11] The $W_2(hpp)_4Cl_2$ compound was previously obtained from a reaction involving WCl_4, $NaHBEt_3$ (1 equiv), and Lihpp (2 equiv) in tetrahydrofuran, in 45% isolated yield.[12] Further reaction of $NaHBEt_3$ with $W_2(hpp)_4Cl_2$ led to $W_2(hpp)_4 \cdot 2NaHBEt_3$ in 38% yield.[13] Furthermore, we have found that the $M_2(hpp)_4$ compounds, **2a** and **2b**, react in chloroform to form their respective "oxidized" $M_2(hpp)_4Cl_2$ compounds, **1a** and **1b**. This ease of oxidation was the focus of a recent report by Cotton and co-workers.[14]

Solid-State and Molecular Structures. Crystals of **1a** and **1b** grown from chloroform solution are isomorphous with six molecules of chloroform per dinuclear unit: $M_2(hpp)_4Cl_2 \cdot 6CDCl_3$. A view of the structure of the tungsten complex **1b** is given in Figure 1. A summary of crystallographic data and selected bond lengths are given in Table 1 and Table 2, respectively.

The compounds $M_2(hpp)_4Cl_2 \cdot 6CDCl_3$ have a crystallographically imposed center of inversion and short metal−metal triple

(3) Chisholm, M. H.; Macintosh, A. M. *J. Chem. Soc., Dalton Trans.* **1999**, 1205−1208.
(4) Cayton, R. H.; Chacon, S. T.; Chisholm, M. H.; Folting, K. *Polyhedron* **1993**, *12*, 415−422.
(5) Chisholm, M. H.; Cotton, F. A.; Daniels, L. M.; Folting, K.; Huffman, J. C.; Iyer, S. S.; Lin, C.; Macintosh, A. M.; Murillo, C. A. *J. Chem. Soc., Dalton Trans.* **1999**, 1387−1392.
(6) Cotton, F. A.; Donahue, J. P.; Lin, C.; Murillo, C. A. *Inorg. Chem.* **2001**, *40*, 1234−1244.
(7) Cotton, F. A.; Lin, C.; Murillo, C. A. *Inorg. Chem.* **2001**, *40*, 575−577.
(8) Cotton, F. A.; Lin, C.; Murillo, C. A. *Inorg. Chem.* **2001**, *40*, 478−484.
(9) Cotton, F. A.; Lin, C.; Murillo, C. A. *Acc. Chem. Res.* **2001**, *34*, 759−771.
(10) Cotton, F. A.; Timmons, D. J. *Polyhedron* **1997**, *17*, 179−184.
(11) Cotton, F. A.; Daniels, L. M.; Murillo, C. A.; Timmons, D. J.; Wilkinson, C. C. *J. Am. Chem. Soc.* **2002**, *124*, 9249−9256.
(12) Clerac, R.; Cotton, F. A.; Daniels, L. M.; Donahue, J. P.; Murillo, C. A.; Timmons, D. J. *Inorg. Chem.* **2000**, *39*, 2581−2584.
(13) Cotton, F. A.; Huang, P.; Murillo, C. A.; Timmons, D. J. *Inorg. Chem. Commun.* **2002**, *5*, 501−504.
(14) Cotton, F. A.; Gruhn, N. E.; Gu, J.; Huang, P.; Lichtenberger, D. L.; Murillo, C. A.; Van Dorn, L. O.; Wilkinson, C. C. *Science (Washington, DC)* **2002**, *298*, 1971−1975.
(15) Chisholm, M. H.; Haitko, D. A.; Folting, K.; Huffman, J. C. *J. Am. Chem. Soc.* **1981**, *103*, 4046−4053.
(16) Chetcuti, M. J.; Chisholm, M. H.; Folting, K.; Haitko, D. A.; Huffman, J. C.; Janos, J. *J. Am. Chem. Soc.* **1983**, *105*, 1163−1170.

Table 1. X-ray Data and Structure Refinement

	1a	**1a**·$6CDCl_3$	**1b**·$6CDCl_3$
empirical formula	$C_{28}H_{48}Cl_2Mo_2N_{12}$	$C_{34}H_{48}Cl_{20}D_6Mo_2N_{12}$	$C_{34}H_{48}Cl_{20}D_6N_{12}W_2$
formula weight	815.56	1537.84	1713.63
temp (K)	150	113	150
wavelength (Å)	0.71073	0.71073	0.71073
crystal system	tetragonal	triclinic	triclinic
space group	*I*4/*m* (No. 87)	*P*-1 (No. 2)	*P*-1 (No. 2)
a (Å)	9.9752(2)	10.3116(4)	10.3837(1)
b (Å)	9.9752(2)	11.1805(4)	11.1668(1)
c (Å)	15.8828(2)	13.2926(5)	13.3458(1)
α (deg)	90	75.7020(10)	75.728(1)
β (deg)	90	81.7050(10)	81.398(1)
γ (deg)	90	85.3730(10)	85.268(1)
V (Å^3)	1580.41(5)	1467.86(10)	1481.17(2)
Z	2	1	1
D_{calc} (gcm^{-3})	1.714	1.740	1.921
abs coeff (mm^{-1})	1.005	1.378	4.822
F(000)	836	766	830
cryst size (mm)	0.15 × 0.15 × 0.08	0.23 × 0.14 × 0.08	0.19 × 0.19 × 0.12
θ range (data collection, deg)	2.41 to 27.47	2.39 to 30.02	2.37 to 27.48
reflections collected	19905	14439	48929
independent reflections	942 [*R*(int) = 0.037]	8498 [*R*(int) = 0.027]	6792 [*R*(int) = 0.056]
data/restraints/parameters	942/5/72	8498/0/425	6792/0/307
goodness-of-fit on F^2	1.137	0.772	1.035
final *R* indices [I > 2*σ*(*I*)]	R1 = 0.0275, wR2 = 0.0706	R1 = 0.0345, wR2 = 0.0576	R1 = 0.0250, wR2 = 0.0554
R indices (all data)	R1 = 0.0311, wR2 = 0.0719	R1 = 0.0566, wR2 = 0.0632	R1 = 0.0317, wR2 = 0.0575
largest diff. peak and hole (eÅ^{-3})	0.556 and −0.384	0.692 and −0.610	1.20 and −0.91

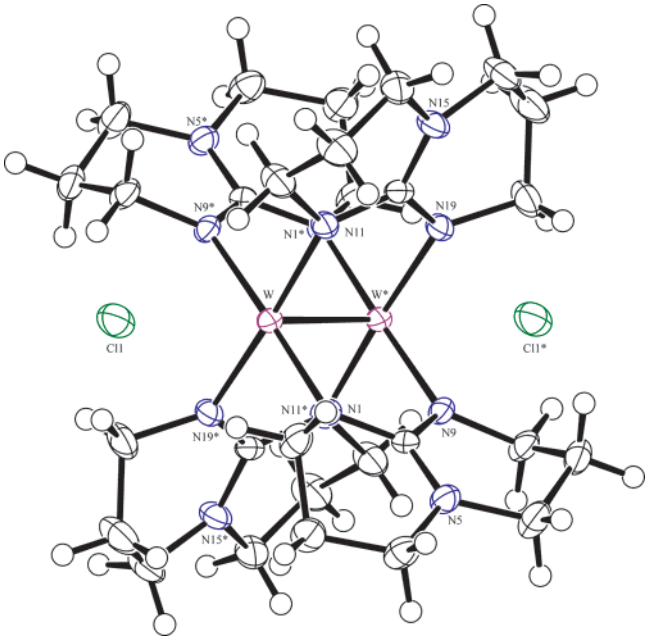

Figure 1. Molecular structure of $W_2(hpp)_4Cl_2$·$6CDCl_3$, with thermal ellipsoids drawn at the 50% probability level. The chloroform molecules have been omitted for clarity.

bond distances, 2.1574(5) Å (M = Mo) and 2.2328(2) Å (M = W). The M−N distances are relatively insensitive to the metal, M−N = 2.09(1) Å (av), and the M−M−N angles are 92° and 91° for M = Mo and W, respectively. For a comparison, it should be noted that in the M−M quadruply bonded compound $Mo_2(hpp)_4$, Mo−Mo = 2.067(1) and Mo−N = 2.16(1) Å (av).[10] The difference of ca. 0.1 Å in M−M distance between closely related M−M triple and quadruple-bonded compounds is typical.[17] The longer Mo−N distances in $Mo_2(hpp)_4$ arise from a combination of factors: (i) the change in the oxidation state of the metals from +2 to +3 is expected to result in a decrease in the M−N bond distances, and (ii) in $Mo_2(hpp)_4$, the M−M *δ* orbital is filled and has a filled−filled (repulsive) interaction with the in-plane N p_π orbitals of the hpp ligand. More of this will be described later. However, by far the most dramatic features of the structures are the presence of the abnormally long M−Cl distances, 3.320(1) Å for M = Mo and 3.212(1) Å for M = W. Moreover, observation of the orientation of the chloroform solvent molecules reveals that each chloride ligand is solvated by three directed hydrogen-bonding interactions from three chloroform molecules that flank the axial site positions. An expanded view of the structure of **1b** clearly showing the solvated chloride ligands is given in Figure 2.

Although M−Cl distances are known to vary significantly with the oxidation state and coordination number of the metal, as well as the *trans* (and to a lesser extent, *cis*) influence of the ligands *trans* (or *cis*) to it, one can safely state that a typical terminal Mo−Cl or W−Cl distance is 2.4(1) Å for Mo or W in the +3 oxidation state. Such distances are seen in, for example, the mononuclear pseudo-octahedral complex *fac*-$WCl_3(PMePh_2)_3$[18] and in the W−W triply bonded compound $W_2Cl_3(NMe_2)_3(PMe_2Ph)_2$. Metal−metal multiple bonds are known to have a high *trans*-influence, and the most closely related compound, $Re_2(hpp)_4Cl_2$, has a similar paddlewheel structure with axial chloride ligands, and a Re−Re quadruple bond (2.1913(2) Å), has Re−Cl = 2.749(5) Å.[19] In reporting the latter distance, Cotton noted that the Re−Cl distance was the longest known for its type of structure. Thus, the Mo−Cl and W−Cl distances reported here, which are ca. 0.5 Å larger, are truly remarkable.

We have also determined the molecular structures of **1a** and **1b** from crystals grown from dichloromethane and found them not to be isomorphous. The molybdenum structure contained no solvent of crystallization, whereas the tungsten structure was

(17) Cotton, F. A.; Walton, R. A. *Multiple Bonds Between Metal Atoms*, 2nd ed.; Oxford University Press: New York, 1993.

(18) Rothfuss, H.; Barry, J. T.; Huffman, J. C.; Caulton, K. G.; Chisholm, M. H. *Inorg. Chem.* **1993**, *32*, 4573−4577.

(19) Cotton, F. A.; Gu, J.; Murillo, C. A.; Timmons, D. J. *J. Chem. Soc., Dalton Trans.* **1999**, 3741−3745.

Table 2. Selected X-ray Structural Data

	M–M (Å)	M–N (Å)	M–Cl (Å)	ref
1a ($Mo_2(hpp)_4Cl_2$)	2.1708(8)	2.10(1) av	3.108(2)	this work
1a·6$CDCl_3$ ($Mo_2(hpp)_4Cl_2$·6$CDCl_3$)	2.1574(5)	2.09(1) av	3.320(1)	this work
1b ($W_2(hpp)_4Cl_2$)	2.250(2)	2.08(1)	3.064(9)	12
1b·6$CDCl_3$ ($W_2(hpp)_4Cl_2$·6$CDCl_3$)	2.2328(2)	2.10(1) av	3.2117(9)	this work
$Mo_2(hpp)_4$	2.067(1)	2.16(1) av	–	10
$W_2(hpp)_4$·2$NaHBEt_3$	2.1608(5)	2.14(1) av	–	13
$Mo_2(hpp)_4(BF_4)_2$	2.142(2)	2.08(1) av	–	20
$Re_2(hpp)_4Cl_2$	2.1931(12)	2.070(7)	2.749(5)	19

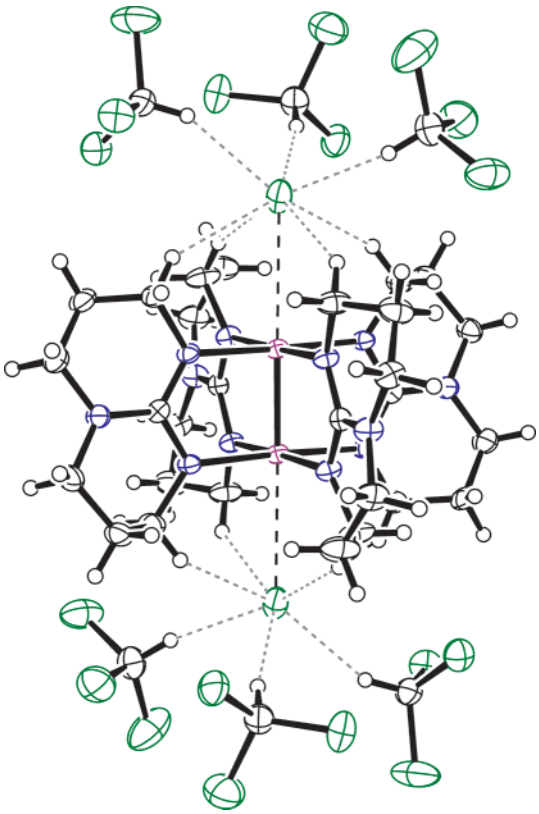

Figure 2. Molecular structure of $W_2(hpp)_4Cl_2$·6$CDCl_3$, showing the chloroform molecules of solvation and all hydrogen bonding as gray dashed lines, with thermal ellipsoids drawn at the 50% probability level.

of the form **1b**·8CH_2Cl_2, with the dichloromethane molecules not involved in hydrogen bonding to the chloride ligands. (The quality of the molecular structure of $W_2(hpp)_4Cl_2$ from CH_2Cl_2, however, was poor, and with the report of the structure of $W_2(hpp)_4Cl_2$ from THF by Cotton,[12] we made no further attempts to refine our determination.) The M−N distances are very similar to those in **1a**·6$CDCl_3$ and **1b**·6$CDCl_3$; however, a slight expansion of the M−M distances to 2.1708(8) Å and 2.250(2) Å[12] for Mo and W, respectively, is observed. That expansion is directly consistent with a corresponding contraction in the M−Cl distances which are notably ca. 0.2 Å shorter at 3.108(2) Å and 3.064(9) Å for Mo and W, respectively.[12] The explanation of these changes in geometry lies solely in the role of the hydrogen bonding of the chloroform molecules to the chloride ligands, stretching the already weak M−Cl bonding. However, one final point of note in the structure of the $M_2(hpp)_4Cl_2$ compounds reported here is that there are eight additional short CH···Cl interactions involving the hpp ligands, four to each Cl (see Figure 2). These CH···Cl interaction imparts a slight twist to the hpp ligands and the paddle-wheel such that

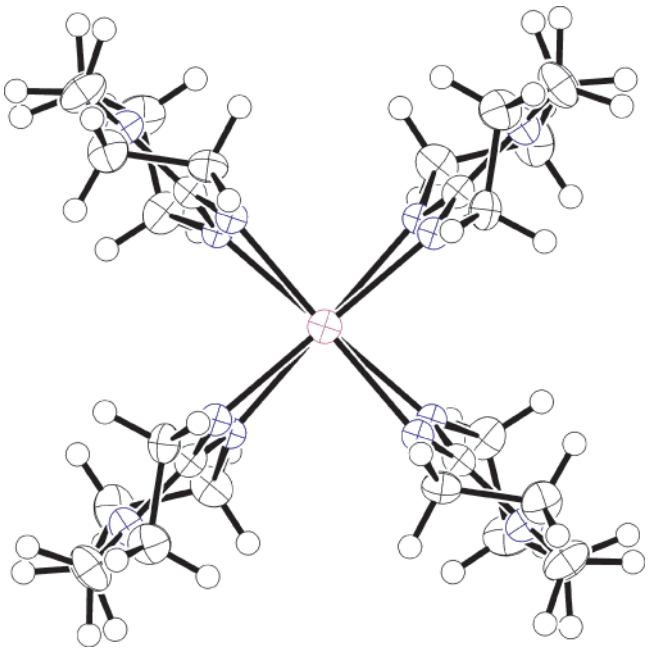

Figure 3. Molecular structure of $Mo_2(hpp)_4Cl_2$ as viewed down the Mo···Mo axis, with thermal ellipsoids drawn at the 50% probability level. The chlorine atoms have been omitted for clarity.

the N−M−M−N dihedral angle is close to 10° as shown in Figure 3. Noteably, such a twist is not seen in the structure of $Mo_2(hpp)_4$ or in the calculated structures of $M_2(hpp)_4$ (see Figure 3) and $M_2(hpp)_4(H)_2$ described later.

A comparison of selected bond distances and bond angles for the structures of **1a** and **1b** reported here, together with those previously reported for $W_2(hpp)_4Cl_2$[12] and the related compounds $Mo_2(hpp)_4$,[10] $W_2(hpp)_4$·2$NaHBEt_3$,[13] $Mo_2(hpp)_4(BF_4)_2$[20] and $Re_2(hpp)_4Cl_2$,[19] are given in Table 2.

The Electronic Structure of $M_2(hpp)_4Cl_2$ and $M_2(hpp)_4$. To investigate the electronic structure and bonding within these dinuclear compounds with abnormally long axial M···Cl distances, we have carried out electronic structure calculations employing density function theory, DFT, using the Gaussian 98 package[21] and the B3LYP functional,[22−24] along with the 6-31G* (5d) basis set for H, C, N, and Cl,[25] and the SDD energy consistent pseudopotentials for molybdenum and tungsten.[26] Geometry optimizations on the atomic coordinates from the X-ray structures of the unsolvated molecules, **1a** and **1b**, were performed under C_1 symmetry. The resulting structures duplicated the observed unsolvated structures very closely with respect to M−M, M−N, and M-Cl distances, and certainly within the small differences expected between solid-state X-ray and gas-phase structures, together with reproducing the twist

(20) Cotton, F. A.; Daniels, L. M.; Murillo, C. A.; Timmons, D. J. *Chem. Commun. (Cambridge)* **1997**, 1449−1450.

Table 3. Calculated Structural Data

	M–M (Å)	M–N (Å)	M–Cl (Å)	M–H (Å)
$Mo_2(hpp)_4Cl_2$	2.218	2.145	2.957	–
$W_2(hpp)_4Cl_2$	2.287	2.147	2.941	–
$Mo_2(hpp)_4$	2.099	2.181	–	–
$W_2(hpp)_4$	2.188	2.172	–	–
$Mo_2(hpp)_4(H)_2$	2.122	2.175	–	1.702
$W_2(hpp)_4(H)_2$	2.197	2.174	–	1.715

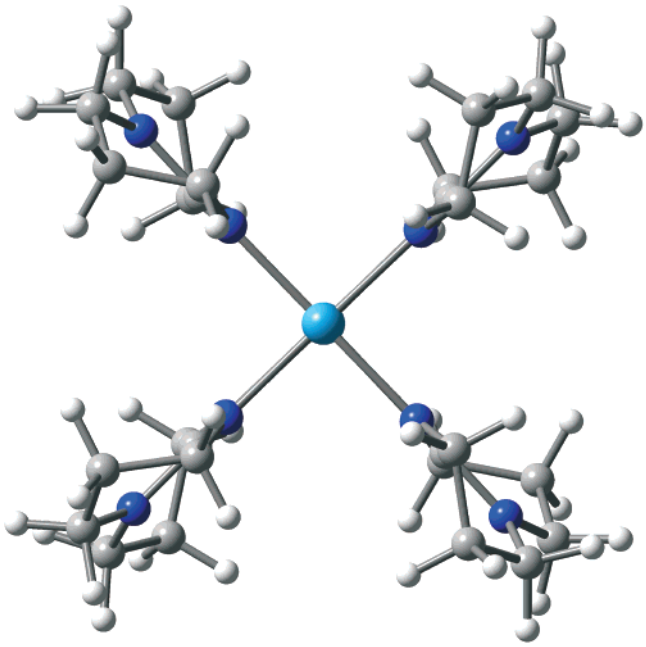

Figure 4. View down the W···W axis of fully relaxed C_1 $W_2(hpp)_4$.

of the four hpp ligands as shown in Figure 3. Calculated gas-phase bond distances for the compounds are given in Table 3. Furthermore, the C_1 gas-phase structures of the related $M_2(hpp)_4$ compounds were determined in similar manners starting from the X-ray determined atomic coordinates of $Mo_2(hpp)_4$.[10] Calculated geometrical parameters for $M_2(hpp)_4$ are also given in Table 3. The calculated structure for $W_2(hpp)_4$ illustrated in Figure 4 agrees well with that recently reported.[13] Note the lack of a twist in the M_2N_8 core of the type described for $M_2(hpp)_4Cl_2$ compounds as shown in Figure 3.

The primary purpose of undertaking these calculations was not, however, to reproduce the observed metrical parameters but rather to gain insight into the abnormally long M−Cl distances and to elucidate the nature of the M−M bonding in the closely related d^3-d^3 $M_2(hpp)_4Cl_2$ and d^4-d^4 $M_2(hpp)_4$ molecules.

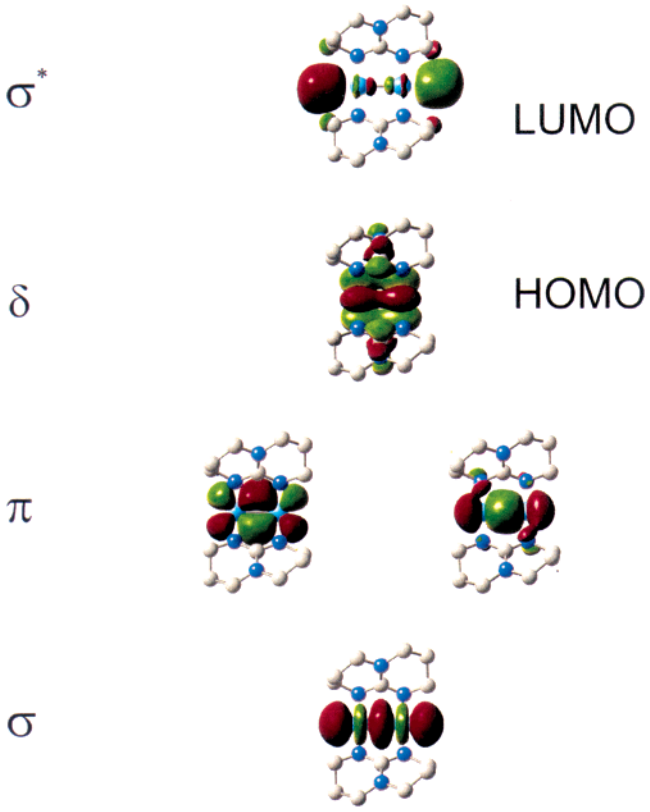

Figure 5. Molecular orbital plots for the M_2-based frontier molecular orbitals of C_1 $W_2(hpp)_4$.

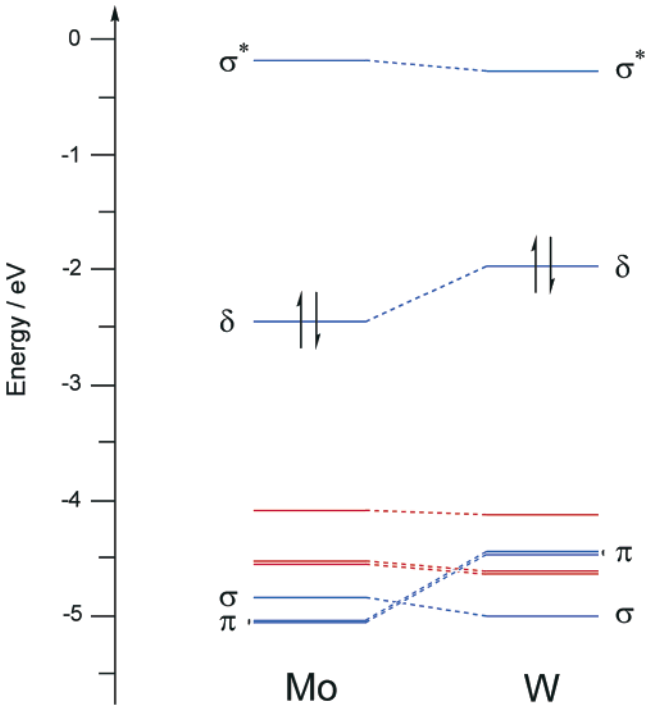

Figure 6. Comparative molecular orbital energy level diagram for C_1 $M_2(hpp)_4$, M = Mo or W. Energy levels drawn in red are ligand N pπ based.

The hpp ligand shows certain similarities to the formamidinate ligands, RNCHNR, and to a first-order approximation, the bonding in $M_2(hpp)_4$ and $M_2(form)_4$,[27] where form = RNCHNR,

(21) Frisch, M. J.; Trucks, G. W.; Schlegel, H. B.; Scuseria, G. E.; Robb, M. A.; Cheeseman, J. R.; Zakrzewski, V. G.; Montgomery, J. A. J.; Stratmann, R. E.; Burant, J. C.; Dapprich, S.; Millam, J. M.; Daniels, A. D.; Kudin, K. N.; Strain, M. C.; Farkas, O.; Tomasi, J.; Barone, V.; Cossi, M.; Cammi, R.; Mennucci, B.; Pomelli, C.; Adamo, C.; Clifford, S.; Ochterski, J.; Petersson, G. A.; Ayala, P. Y.; Cui, Q.; Morokuma, K.; Malick, D. K.; Rabuck, A. D.; Raghavachari, K.; Foresman, J. B.; Cioslowski, J.; Ortiz, J. V.; Baboul, A. G.; Stefanov, B. B.; Liu, G.; Liashenko, A.; Piskorz, P.; Komaromi, I.; Gomperts, R. J.; Martin, R. L.; Fox, D. J.; Keith, T.; Al-Laham, M. A.; Peng, C. Y.; Nanayakkara, A.; Challacombe, M.; Gill, P. M. W.; Johnson, B.; Chen, W.; Wong, M. W.; Andres, J. L.; Gonzalez, C.; Head-Gordon, M.; Replogle, E. S.; Pople, J. A. *Gaussian 98*, Version A9; Gaussian Inc.: Pittsburgh, PA, 1998.
(22) Becke, A. D. *Phys. Rev. A: Gen. Phys.* **1988**, *38*, 3098−3100.
(23) Becke, A. D. *J. Chem. Phys.* **1993**, *98*, 5648−5652.
(24) Lee, C.; Yang, W.; Parr, R. G. *Phys. Rev. B: Condens. Matter* **1988**, *37*, 785−789.
(25) Hehre, W. J.; Radom, L.; Schleyer, P. v. R.; Pople, J. A. *Ab initio Molecular Orbital Theory*; John Wiley & Sons: New York, 1986.
(26) Andrae, D.; Haeussermann, U.; Dolg, M.; Stoll, H.; Preuss, H. *Theor. Chim. Acta* **1990**, *77*, 123−141.

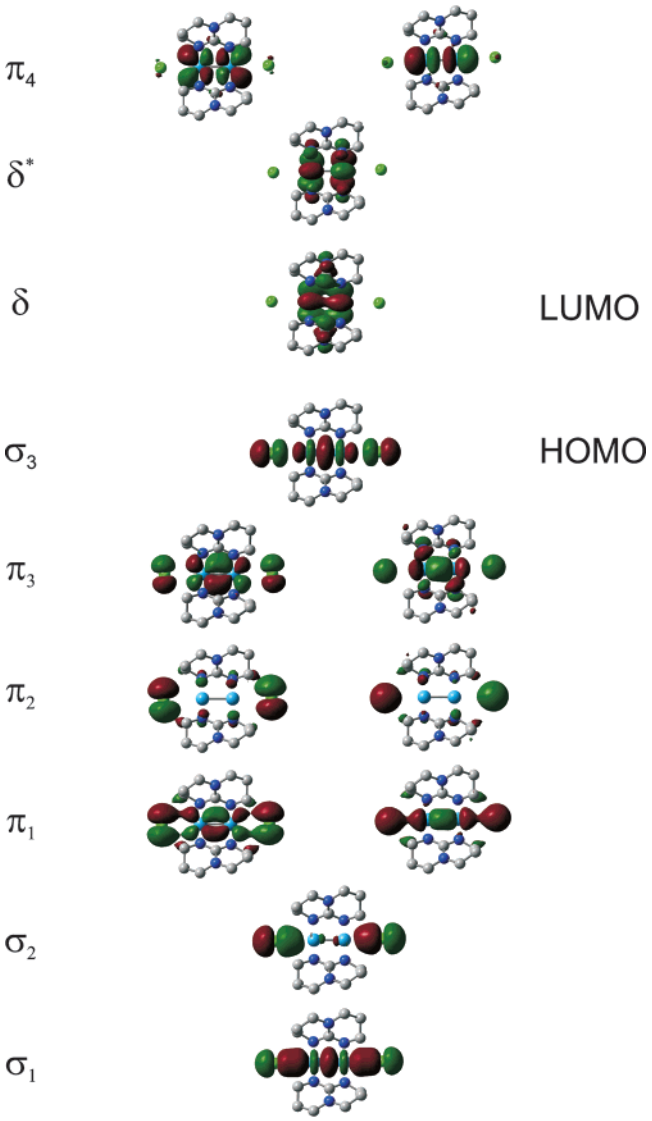

Figure 7. Molecular orbital plots for the M_2Cl_2-based frontier molecular orbitals of C_1 $W_2(hpp)_4Cl_2$.

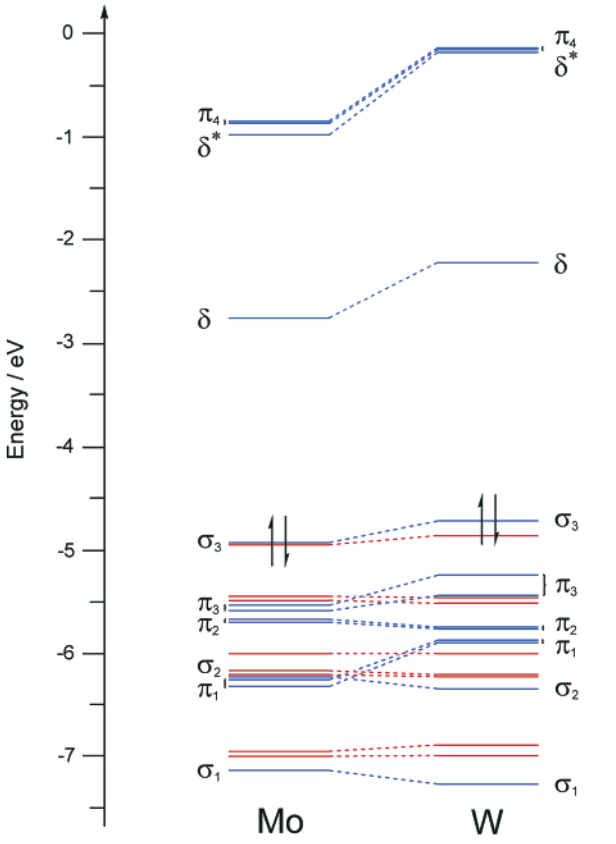

Figure 8. Comparative molecular orbital energy level diagram for C_1 $M_2(hpp)_4Cl_2$, M = Mo or W. Energy levels drawn in red are ligand N pπ based.

are very similar. The HOMO has M−M δ character as can be seen from the frontier molecular orbital representations for $W_2(hpp)_4$ shown in Figure 5. As in $M_2(form)_4$ compounds,[27] there is extensive mixing of the M−M π and ligand N p_π sets of orbitals which lie directly below this in energy. A molecular orbital energy level diagram for the frontier molecular orbitals of the $M_2(hpp)_4$ molecules is given in Figure 6, which allows a comparison of the related energies of equivalent MOs for $Mo_2(hpp)_4$ and $W_2(hpp)_4$. Suffice it to state that these molecules can be conceived as having M−M quadruple bonds. Note too that the high δ orbital energy, which is also more than 1.5 eV higher than that of the HOMO-1 in each case, implies that these molecules might be very easily ionized to their respective cations, and indeed, this was recently demonstrated by Cotton and co-workers who found the first ionization energy of $W_2(hpp)_4$ to be less than the cesium atom.[14] The authors also offered an explanation of the behavior based on calculations.

The bonding in the $M_2(hpp)_4Cl_2$ compounds is more complex. However, the most important feature in the electronic structure calculation is that the HOMO is found to be M−M σ and M−Cl σ* in character as shown in the frontier molecular orbital plots of $W_2(hpp)_4Cl_2$ given in Figure 7. A molecular orbital energy level diagram for the frontier molecular orbitals of the $M_2(hpp)_4Cl_2$ molecules comparing molybdenum and tungsten is given in Figure 8.

Given the experimentally observed, abnormally long (and presumably labile) axial ligands in $M_2(hpp)_4Cl_2$ molecules and that the computations duplicate these structures and reveal that the HOMO is M−M σ bonding but strongly M−Cl σ antibonding, one has good reason to question whether compounds of the type $M_2(hpp)_4(X)_2$ where X is a ligand with a high *trans*-influence, such as alkynyl (−C≡CR), could exist. These would be essential for the success of any synthetic strategy aimed at preparing oligomers of the type $[M_2(hpp)_4(C{\equiv}C)]_n$ noted in the introduction. In an attempt to investigate this problem from a theoretical standpoint, we undertook calculations on the hypothetical dihydrido molecules $M_2(hpp)_4(H)_2$ where the M−H bond assumed an axial site and modeled related hydrocarbyl ligands such as −C≡CR which are known to exert a high *trans*-influence. In these calculations, the chloride ligands of $M_2(hpp)_4Cl_2$ were replaced by hydride ligands with a starting M−H distance of 2.20 Å, and the geometries reoptimized. The resulting structure of $Mo_2(hpp)_4(H)_2$ is shown in Figure 9, and the calculated M−M, M−N, and M−H distances are given in Table 3. The four hpp ligands adopt a regular paddle-wheel geometry, and rather interestingly, the calculated structures show short M−M distances (for triple bonds between d^3−d^3 Mo_2 and W_2 units), but somewhat lengthened M−N bond distances. A

(27) Lichtenberger, D. L.; Lynn, M. A.; Chisholm, M. H. *J. Am. Chem. Soc.* **1999**, *121*, 12167−12176.

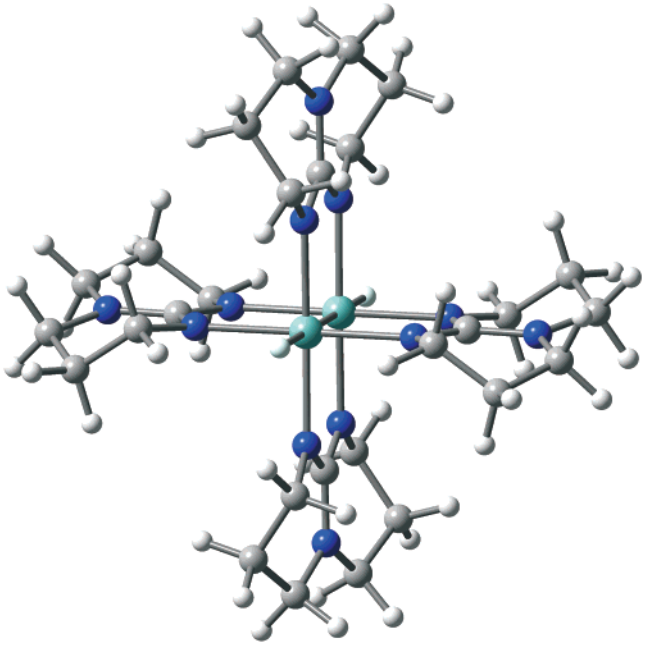

Figure 9. View of fully relaxed C_1 $Mo_2(hpp)_4(H)_2$.

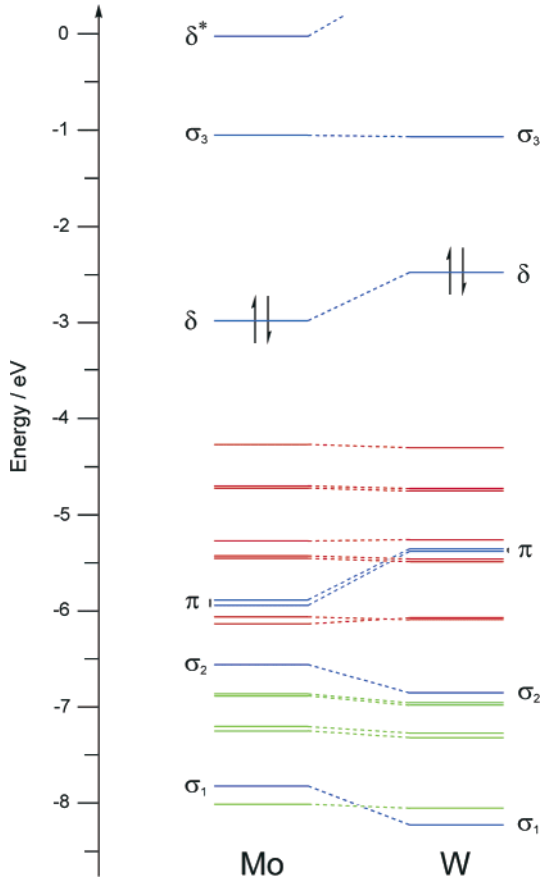

Figure 10. Comparative molecular orbital energy level diagram for C_1 $M_2(hpp)_4(H)_2$, M = Mo or W. Energy levels drawn in red are ligand N pπ based, and those in green are M−N σ based.

molecular orbital energy level diagram for the frontier orbitals of the $M_2(hpp)_4(H)_2$ molecules is given in Figure 10. The HOMO is M−M δ with some M−C π* mixing. The LUMO is M−M σ and strongly M−H σ* in character, being almost exclusively metal d_{z^2} and H 1s in character. Orbital representations of the frontier molecular orbitals of $Mo_2(hpp)_4(H)_2$ are given in Figure 11. Somewhat below the HOMO come the M−M π molecular orbitals which mix extensively with the ligand N−C p_π orbitals. There is a close relationship with the bonding described previously for $W_2(O_2CR)_4(R')_2$ compounds, which have axially ligated R′ groups (R′ = Me, Ph, CH_2Ph, and $CH_2{}^tBu$), for which the M−M bonding configuration of $\pi^4\delta^2$ was given for the formal d^3−d^3 triple bond.[28] Note also in comparing the bonding in the $M_2(hpp)_4X_2$ molecules, where X = Cl and H (Figures 8 and 10), it is principally the relative energy of the σ_3 MO that changes.

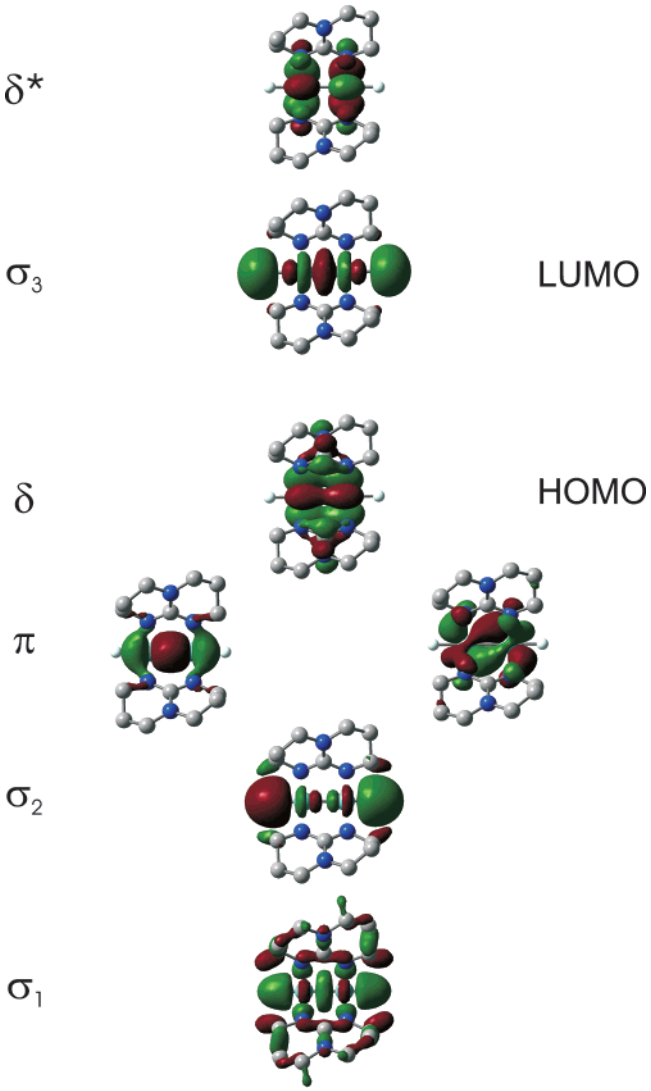

Figure 11. Molecular orbital plots for the M_2H_2-based frontier molecular orbitals of C_1 $Mo_2(hpp)_4(H)_2$.

The bonding in the $M_2(hpp)_4$, $M_2(hpp)_4(H)_2$, and $M_2(hpp)_4Cl_2$ molecules and the simple organic molecules C_2, C_2H_2 (acetylene), and C_2Cl_2 (dichloroacetylene) provide most interesting comparisons of inorganic and organic multiple bonds as we show below from the results of further DFT calculations (see Experimental Section for details).

C_2, C_2H_2, and C_2Cl_2. The diatomic molecule C_2 is well-known to be an example of a molecule having a formal double

(28) Chisholm, M. H.; Clark, D. L.; Huffman, J. C.; Van der Sluys, W. G.; Kober, E. M.; Lichtenberger, D. L.; Bursten, B. E. *J. Am. Chem. Soc.* **1987**, *109*, 6796−6816.

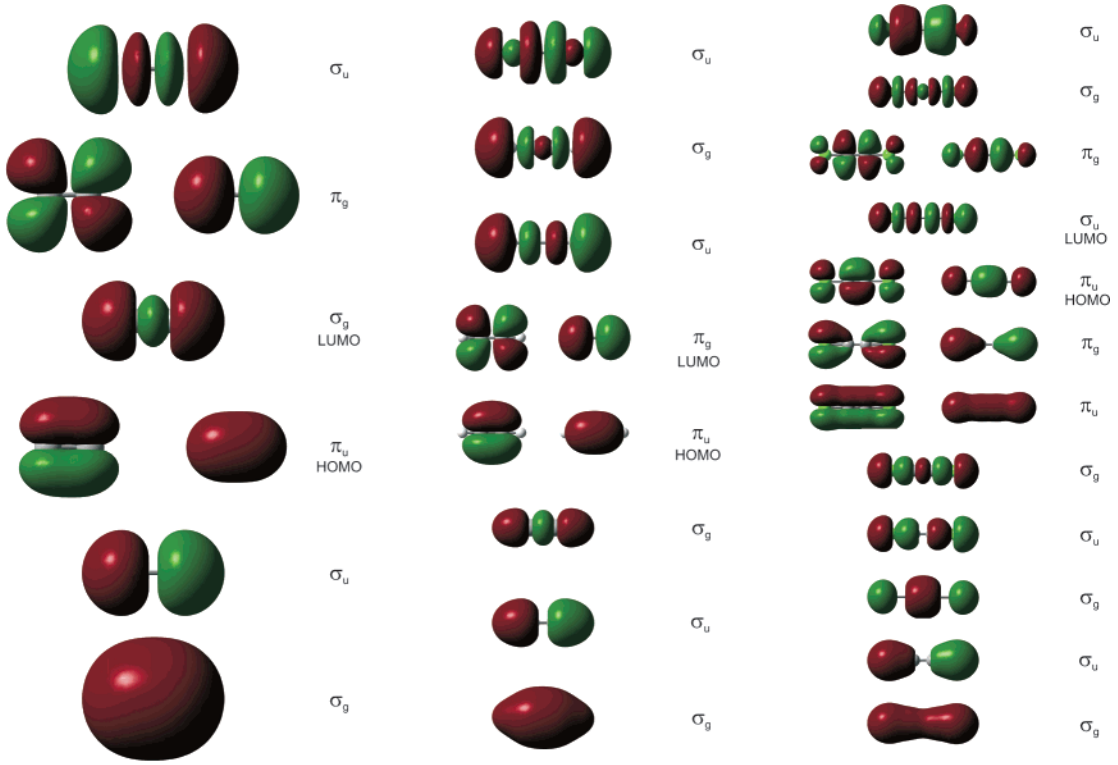

Figure 12. Molecular orbital plots for the frontier molecular orbitals of $D_{\infty h}$ C_2 (left), C_2H_2 (center), and C_2Cl_2 (right).

bond of configuration π^4.[29] However, as a result of sp mixing between carbons 2s and 2p orbitals, there is residual net σ bonding, and the LUMO is only weakly C−C bonding.[30] The orbital plots calculated for C_2 are shown in Figure 12.

The bonding in acetylene can be viewed as a result of the interaction of two H atoms with the C_2 molecule to form linear HCCH. The in-phase combination of H atoms finds a symmetry match with the lowest-energy molecular orbital and the LUMO, both of which have σ_g symmetry. These combine to form two bonding σ_g orbitals, one of which, the lowest-energy one, is mostly C−C with some C−H σ bonding and the other more C−H but with some C−C bonding. The out-of-phase combination of the H 1s orbitals leads to an occupied orbital which is strongly C−H bonding with little C−C σ^* character and an unoccupied totally antibonding orbital of σ_u symmetry which is entirely C−H and C−C σ^* in character. The HOMO is the doubly degenerate π_x π_y bonding molecular orbital, π_u, and the LUMO is π_g, the antibonding counterparts. These orbitals are illustrated in Figure 12.

The dichloroacetylene molecule has the remnants of the H−C−C−H σ bonding framework, but with Cl 3p atomic and Cl 3s mixing, there are now eight σ molecular orbitals. The C_2 p_π atomic orbitals mix extensively with the Cl 3p which are of a similar energy. This results in the formation of eight π MOs. The σ and π MOs for ClCCCl are shown in Figure 12. The lowest-energy molecular orbitals are σ in character and use predominantly Cl 3s and C 2s but with some p mixing.

Five σ orbitals are occupied. The lowest in energy is totally symmetric and C−Cl and C−C bonding. The next is predominantly C−Cl bonding but with Cl lone-pair character, followed by the third which is C−C σ bonding with Cl lone-pair character. The fourth has three nodes and may be considered as predominantly nonbonding, while the fifth, and highest occupied, has four nodes and is σ bonding (being equivalent in symmetry to the alignment of four p_z atomic orbitals with in-phase combinations) but with some additional Cl lone-pair character. The π set are represented by four sets of doubly degenerate orbitals. The lowest in energy is totally C−C and C−Cl π bonding. The second is C−Cl π bonding and weakly C−C π antibonding, π_g. The third is C−C π bonding but C−Cl π^* in character, π_g, and the fourth and highest-energy MO is predominantly C−C and C−Cl π^* with some Cl lone-pair character, π_g.

With 22 valence electrons, the HOMO is the C−C π MO with weak Cl−C π^*, or Cl p_π lone-pair character. The LUMO is Cl−C σ bonding and C−C σ^* in character. The linear $[Cl-M-M-Cl]^{4+}$ moiety that is contained within the $M_2(hpp)_4Cl_2$ molecules also has 22 valence electrons, and the similarities and differences between the inorganic and organic σ and π systems can be seen by a comparison of the orbital plots shown in Figures 7 and 12.

Concluding Remarks

The compounds of formula $M_2(hpp)_4Cl_2$ have abnormally long M−Cl distances as a result of a new type of M−M configuration for a d^3-d^3 triple bond, namely $\pi^4\sigma^2$ where the HOMO is M−M σ bonding and M−Cl antibonding. Does this mean that compounds of formula $M_2(hpp)_4(C{\equiv}CR)_2$ and oligomers of the type shown in **V** will be inaccessible and labile to reductive elimination even though related $[Ru_2]-(C{\equiv}CR)_2$[31] and $(RC{\equiv}C)-[Ru_2]-(C{\equiv}C-C_6H_4-C{\equiv}C)-[Ru_2]-(C{\equiv}CR)$

(29) Gray, H. B.; DeKock, R. L. *Chem. Struct. Bonding* 1980.
(30) Mulliken, R. S.; Ermler, W. C. *Diatomic Molecules. Results of ab Initio Calculations*; Academic Press: New York, 1978.
(31) Li, Y.; Han, B.; Kadish, K. M.; Bear, J. L. *Inorg. Chem.* **1993**, *32*, 4175−4176.

compounds[32] are known? We have calculated the enthalpy changes associated with the hypothetical reactions shown in **VI**.

$$M_2(hpp)_4 + X_2 \rightarrow M_2(hpp)_4(X)_2 \qquad \textbf{VI}$$

For X = Cl, the reactions are calculated to be exothermic by 96 kcal mol^{-1} for molybdenum and 122 kcal mol^{-1} for tungsten. However, for X = H, the reactions are endothermic by 30 and 20 kcal mol^{-1} for molybdenum and tungsten, respectively. This, together with the observed preparation of $M_2(hpp)_4$ in the dealkylation reactions described in this work, suggests that linear compounds containing the connectivity −(C≡C)−M≡M−(C≡C)− (M = Mo or W) may be unattainable.

Experimental Section

General Procedures. Due to the air-sensitive nature of the materials, all were synthesized and manipulated under dinitrogen or argon atmospheres using either standard Schlenk-line or drybox techniques. Solvents were predried over activated molecular sieves, refluxed over calcium hydride (protio- and deuterodichloromethane and chloroform) or molten potassium (protio- and deuterobenzene) under an atmosphere of dinitrogen, collected by distillation, and then degassed. The compounds 1,2-$M_2Cl_2(NMe_2)_4$[33] and 1,2-$M_2R_2(NMe_2)_4$[15,16] (M = Mo or W, R = ^{i}Bu or *p*-tolyl) were prepared as previously described. 1,3,4,6,7,8-Hexahydro-2*H*-pyrimido[1,2-*a*]pyrimidine, Hhpp, was purchased from Aldrich and sublimed prior to use.

$M_2(hpp)_4Cl_2$ (1a M = Mo, 1b M = W). Inside a glovebox, 1,2-$M_2Cl_2(NMe_2)_4$ (1.00 mmol, 439 mg M = Mo, 614 mg M = W) were placed together with Hhpp (8.00 mmol, 1.11 g) in a pestle and mortar and finely ground and then placed in a sublimation apparatus. The orange mixture was then heated under an argon atmosphere at 150 °C overnight (12 h; M = Mo, 15 h; M = W) during which time the color of the mixture changed to brown, and $HNMe_2$ was evolved and allowed to escape through a non-return bubbler. On cooling, the apparatus was evacuated to 10^{-3} Torr, the mixture was returned to the drybox, and the resulting solid mass was then finely powdered. Sublimation at ca. 150 °C, 10^{-4} Torr, then removed the excess Hhpp and any other residual volatiles. Subsequent recrystallization from dichloromethane gave $Mo_2(hpp)_4Cl_2$, **1a** (775 mg, 95%), or $W_2(hpp)_4Cl_2$, **1b** (970 mg, 98%). Note well: the melt reactions were subsequently shown to give $M_2(hpp)_4Cl_2$ in essentially quantitative yield by ^{1}H NMR spectroscopy. $Mo_2(hpp)_4Cl_2$, **1a**:^{1}H NMR ($CDCl_3$, 298 K): δ 3.34 (t, 16 H, CH_2), 3.30 (t, 16 H, CH_2), 2.01 (quin, 16 H, CH_2). Anal. Found (calcd) for $C_{18}H_{48}Cl_2Mo_2N_{12}$: C, 41.01 (41.24); H, 5.95 (5.93); N, 20.23 (20.61). $W_2(hpp)_4Cl_2$, **1b**:^{1}H NMR ($CDCl_3$, 298 K): δ 3.36 (t, 16 H, CH_2), 3.30 (t, 16 H, CH_2), 12.03 (quin, 16 H, CH_2). Anal. Found (calcd) for $C_{18}H_{48}Cl_2N_{12}W_2$: C, 33.48 (33.92); H, 4.80 (4.88); N, 16.67 (16.95).

$M_2(hpp)_4$ (2a M = Mo, 2b M = W). Inside a glovebox, 1,2-$W_2R_2(NMe_2)_4$ (0.400 mmol, 264 mg R = ^{i}Bu; 290 mg R = *p*-tolyl) was combined with Hhpp (1.600 mmol, 222 mg) and a magnetic stirrer bar in a Schlenk tube. On removal from the drybox, dry benzene (25 mL) was added, and the resulting orange mixture was stirred for 3 days under an argon atmosphere. The volatiles were removed from the then yellow solution and the resulting yellow powder thoroughly dried to 10^{-3} Torr. The crude product was then dissolved in the minimum dry benzene before precipitation by the addition of dry hexane, subsequent filtration, washing with hexane, and thoroughly dried to afford $W_2(hpp)_4$ **2b** (R = ^{i}Bu; 365 mg, 99%, R = *p*-tolyl; 342 mg, 93%). ^{1}H NMR (C_6D_6, 298 K): δ 3.28 (t, 16 H, CH_2), 3.22 (t, 16 H, CH_2), 1.95 (quin, 16 H, CH_2). Anal. Found (calcd) for $C_{18}H_{48}N_{12}W_2$: C, 36.34 (36.54); H, 5.40 (5.26); N, 18.20 (18.26).

Experiments carried out in NMR tubes in C_6D_6 confirmed that for R = Bu isobutane and isobutylene are eliminated and, where R = *p*-tolyl, the volatile biaryl product of coupling is produced. Similarly, reactions employing 1,2-$Mo_2R_2(NMe_2)_4$ (R = ^{i}Bu or R = *p*-tolyl) and 4 equiv of Hhpp over several days afforded $Mo_2(hpp)_4$ as confirmed by comparison to a sample made by the literature procedure.[10,11]

X-ray Structure Determinations. 1a. A dark brown transparent crystal grown from dichloromethane solution was transferred to a pool of Paratone N oil and then mounted onto a glass fiber and transferred to the goniostat where it was cooled to 150 K for characterization and data collection using an Oxford Cryosystems Cryostream cooler. Examination of the diffraction pattern on a Nonius Kappa CCD diffractometer indicated an I-centered tetragonal crystal system, and thus an octant of data was collected. Data integration was performed with Denzo,[34] and an empirical absorption correction was applied with Sortav.[35] The structure can be solved by the Patterson method in SHELXS-86[36] in the three possible space groups *I*4, *I*-4, and *I*4/*m*, with a consistently disordered hpp ligand. Full-matrix least-squares refinements based on F^2 were performed in SHELXL-93[37] in the *I*4/*m* space group. The complex contains crystallographic 4/*m* symmetry, with the Mo−Mo bond lying along the four-fold axis and bisected by the mirror plane. As a result, the asymmetric unit consists of one Mo atom, one Cl atom, and half of an hpp ligand. Disorder in the ligands was modeled with two positions for the N(1), C(2), and C(3) atoms, each with an occupancy factor of 0.5. All of the non-hydrogen atoms, with the exception of N(l) and N(1A), were refined anisotropically. Bond length restraints were applied to the disordered region of the ligands. The following pairs of bond lengths were restrained to be equal: N(1)−C(10) and N(1A)−C(10), N(1)−C(2) and N(1A)−C(2A), C(2)−C(3) and C(2A)−C(3A), C(3A)−C(4) and C(3)−C(4), Mo−N(1) and Mo−N(1A). The hydrogen atoms were included in the model at calculated positions using a riding model. The final difference electron density map contains maximum and minimum peak heights of 0.56 and −0.38 e$^-$Å^3. Neutral atom scattering factors were used and include terms for anomalous dispersion.[38]

1a·6CDCl$_3$. A pale brown−green transparent crystal ground from deuterated chloroform solution was mounted under an inert atmosphere onto a glass fiber using silicone grease and transferred to the goniostat, where it was cooled to −160 °C for characterization and data collection using a gas-flow cooling system of local design. A systematic search of a limited hemisphere of reciprocal space was used to determine that the crystal possessed no symmetry or systematic absences indicating a triclinic space group. Subsequent solution and refinement confirmed this choice. The data were collected using a Bruker-AXS SMART6000 CCD area detector system utilizing the SMART software,[39] and integrated intensities corrected for Lorentz and polarization effects as well as absorption were obtained using the SAINT software.[40] The structure was solved by direct methods (MULTAN78) and Fourier techniques. Hydrogen atoms were located in a difference Fourier and refined isotropically in the final cycles of refinement. The hydrogen atoms associated with C(18) converged to unrealistic positions, and examination indicated that the largest peak in the difference electron density map (0.92 e$^-$Å^3) was in fact, a partial occupancy carbon. When the alternate position was included, the occupancy refined to 15:85, and the hydrogen atoms, when adjusted to the proper occupancy, refined reasonably. The final difference electron density map was featureless, the largest peak being 0.46 e$^-$Å^3, lying at the origin between the two metal atoms.

(32) Wong, K.-T.; Lehn, J.-M.; Peng, S.-M.; Lee, G.-H. *Chem. Commun. (Cambridge)* **2000**, 2259−2260.
(33) Akiyama, M.; Chisholm, M. H.; Cotton, F. A.; Extine, M. W.; Murillo, C. A. *Inorg. Chem.* **1977**, *16*, 2407−2411.
(34) Otwinowski, Z.; Minor, W. *Methods Enzymol.* **1997**, *276*, 307−326.
(35) Blessing, R. H. *Acta Crystallogr., Sect. A* **1995**, *A51*, 33−38.
(36) Sheldrick, G. M. *Acta Crystallographica, Section A: Foundations of Crystallography* **1990**, *A46*, 467−473.
(37) Sheldrick, G. M. *SHELXL-93*; University of Gottingen: Germany, 1993.
(38) *International Tables for Crystallography*; Kluwer Academic Publishers: Dordrecht, 1992; Vol. C.
(39) *SMART*; Bruker Analytical X-ray Systems: Madison, WI, 1996.
(40) *SAINT*; Bruker Analytical X-ray Systems: Madison, WI, 1996.

1b·6CDCl$_3$. A dark-brown transparent crystal grown from deuterated chloroform solution was transferred to a pool of Paratone N oil and then mounted onto a glass fiber and transferred to the goniostat, where it was cooled to 150 K for characterization and data collection using an Oxford Cryosystems Cryostream cooler. Examination of the diffraction pattern on a Nonius Kappa CCD diffractometer indicated a triclinic crystal system, and so a hemisphere of data was collected. Data integration was performed with Denzo,[34] and an empirical absorption correction was applied with Sortav.[35] The structure was solved by the Patterson method in SHELXS-86.[36] Full-matrix least-squares refinements based on F^2 were performed in SHELXL-93.[37] The hydrogen atoms were included in the model at calculated positions using a riding model. The final difference electron density map contains maximum and minimum peak heights of 1.20 and −0.91 e$^-$Å^3. Neutral atom scattering factors were used and include terms for anomalous dispersion.[38]

Molecular and Electronic Structure Calculations. Molecular and electronic structure determinations on the compounds $M_2(hpp)_4Cl_2$, $M_2(hpp)_4$, and $M_2(hpp)_4(H)_2$ (M = Mo or W) were performed employing density function theory, DFT, using the Gaussian 98 package[21] and the B3LYP functional,[22−24] along with the 6-31G* (5d) basis set for H, C, N, and Cl,[25] and the SDD energy consistent pseudopotentials for molybdenum and tungsten.[26] Geometry optimizations were performed under C_1 symmetry on either the atomic coordinates from the respective X-ray structures or after direct adaptation of the previously optimized parent species as described in the text. All geometries were fully optimized under the default optimization criteria of the program. The geometries and electronic structures of C_2, C_2H_2, and C_2Cl_2 were optimized at the 6-31G* (5d) level for H, C, and Cl. Orbital analyses were completed with *GaussView*.[41]

Acknowledgment. We thank the National Science Foundation for financial support, and the Ohio Supercomputer Center is gratefully acknowledged for computational resources with which the DFT calculations were performed. We also thank the reviewers for their constructive comments.

Supporting Information Available: Full X-ray structural information on **1a**, **1a·6CDCl$_3$**, and **1b·6CDCl$_3$** are available as an X-ray crystallographic file in CIF format. This material is available free of charge via the Internet at http://pubs.acs.org. CIFs have been submitted to the CCDC with entry numbers CCDC 220629−220631 for **1a**, **1a·6CDCl$_3$**, and **1b·6CDCl$_3$**, respectively.

JA0301065

(41) *GaussView 2.1*; Gaussian Inc.: Pittsburgh, PA, 1998.